European Journal of Molecular & Clinical Medicine
ISSN 2515-8260 Volume 07, Issue 05, 2020

# LIKELIHOOD BASED PROBABILITY DENSITY FUNCTION WITH RELEVANCE VECTOR MACHINE AND GROWING CONVOLUTION NEURAL NETWORK FOR AUTOMATIC BRAIN TUMOR SEGMENTATION

B. Devanathan[1], Dr. K. Venkatachalapathy[2]

[1]*Research Scholar, Department of Computer and Information Science, Annamalai University, Chidambaram, India.*

[2]*Professor, Department of Computer and Information Science, Annamalai University, Chidambaram, India.*

[1]*devacisau@gmail.com*

[2]*omsumeetha@rediffmail.com*

*Abstract**: Brain tumor (BT) segmentation is a significant process in clinical imaging. Earlier identification of BT acts as a crucial process to improve the treatment prospects and enhances the endurance rate of the patients. Manual segmentation of the BTs for cancer detection from enormous quantity of MRI images produced in a daily medical schedule is a troublesome and tedious process. Therefore, an automated BT segmentation tool is required. In this view, this paper presents a novel Likelihood based Probability Density Function with Relevance Vector Machine (LPDF-RVM) and Growing Convolution Neural Network (GCNN) for automatic BT segmentation. Initially, MR brain images are taken as input. In addition, the image normalization process and wiener filter based noise removal process takes place along with the skull stripping process. After that, Gray-Level Co-Occurrence Matrix (GLCM) and Histogram of Oriented Gradients (HOG) features extraction is performed. Based on the features, LPDF-RVM is applied as a segmentation technique followed by GCNN. A detailed simulation analysis was carried out to highlight the better performance of the presented model.***

***Keywords: BT segmentation, MR images, HOG and GLCM***

## 1. INTRODUCTION:

Recently, Brain tumor (BT) is the most dangerous disease arising generally among human beings [1]. BT is an unrestrained situation of brain which leads to the creating of abnormal group of cells in brain or neighboring it. During this development of abnormal cells abrupt the normal procedure of the brain and it contains adverse results on patient's health [2]. It has 2 kinds of BTs such as primary tumor and secondary or metastatic tumor [3]. Usually, the primary BT outsets in the brain and tends to stay during its growth tenure [4]. Whereas, the secondary BT commences elsewhere as cancer in the body and later spreads to the brain region.

Diverse clinical imaging strategies and techniques that incorporate, for example, Computed Tomography (CT), Single-Photon Emission Computed Tomography (SPECT), Positron Emission Tomography (PET), Magnetic Resonance Spectroscopy (MRS), and Magnetic Resonance Imaging (MRI) are completely utilized for providing the significant data on shape, size, area, and metabolism of BTs aiding in identification [5]. But, these modalities are utilized to mix for giving the most elevated data on BTs, because of its soft tissue contrast, and generally accessible MRI is regarded as the usual strategy.

The MRI is a non-obtrusive in vivo imaging method which utilizes radio signal to energize target tissues for producing their inner images affected by a magnetic field. Images of various MRI groupings are created by adjusting the excitation and reiteration times in the picture collection process [6-8]. These diverse MRI systems produce various kinds of tissue contrast images, in this manner giving important primary data and empowering analysis and division of tumors alongside their sub-regions. Different kinds of image processing (IP) strategies and techniques are utilized to determine and treatment of a BT. In segmentation is the essential advance in IP strategies and is utilized to remove the contaminated area of cerebrum tissue from MRIs. The segmentation of the tumor area is a significant undertaking to determination, treatment, and the assessment of treatment results. Numerous strategies, for example, Fuzzy C-Means (FCM), Support Vector Machine (SVM), Artificial Neural Network (ANN), information depends on methods, and Expectation-Maximization (EM) have been proposed for characterization of BTs in MR images.

[9] developed an extended edge prediction approach BT segmentation. The automated image based thresholding has been deployed which is combined with Sobel operator for edge prediction in BT. Then, tumor region is isolated by applying closed contour algorithm as well as object separation based segmentation. The simulation outcome of presented model is optimal when compared with classical model. [10] developed a multi-phase system for BT classification. In this work, there are 2 phases namely, BT analysis and tumor extraction. Initially, BT diagnosis is attributed to extract texture features from noise free brain MRI images. Ensemble relied on SVM classifier that has been applied for tumor classification. Secondly, tumor extraction, skull elimination, brain extraction as well as BT extraction has been performed for BT classification.

[11] developed a mesh-free total Lagrangian explicit dynamic (TLED) method for dealing the simulation with atlas distortion and applied the structure of tumor segregated from multimodal MRI for deriving a novel development approach. Then, it is applicable for handling huge deformation with no remeshing. Therefore, tumor development methods apply original shape of tumor rather than using irregular shapes and need no seed simulation. Hence, the model enhances the efficiency of parameter difference and limited the processing time interms of parallel computation. The merits of this model are to perform image segmentation with better correlation among pixels and region intensities. The major limitations of atlas relied upon segmentation which needs maximum computation time for atlas development. [12] projected a fuzzy model for BT prediction in multispectral, T1-weighted magnetic resonance, weighted T2 weights, as well as proton density for image segmentation. Some of the models applied in this study are multispectral MRI records. Then, data is collected from intensity of an image. This data can be applied for fuzzy automation and depicted as a parameter. Lastly, fuzzy image segmentation becomes valuable for gaining resultant image. As a result, the projected model is composed of massive benefits like segmentation of the 3D image, and this segmentation applies the pathological data.

[13] deployed a Deep Learning (DL) based enhanced tumor segmentation for MR brain images. Here, input image is pre-processed prior to compute segmentation. Firstly,

normalization of input image is performed and proceed with further process. Then, WF is employed for noise elimination and compute the blurred images. Next, skull stripping is carried out for eliminating the skull from MRI image with the help of traversal graph scheme. It is also a 2-phase framework. When the region of interest (ROI) is found, feature extraction is processed under the application of Stationary Wavelet Transform (SWT). Hence, SWT performs better when compared with Fourier models since the wavelets are applied for data with irregularities. Next, GCNN is applied for training and classification of healthy and anomalous patient [16-21].

This paper presents a novel Likelihood based Probability Density Function with Relevance Vector Machine (LPDF-RVM) and Growing Convolutional Neural Network (GCNN) for automatic BT segmentation. Initially, MR brain images are taken as input. In addition, the image normalization process and wiener filter (WF) based noise removal process takes place along with the skull stripping process. After that, Gray-Level Co-Occurrence Matrix (GLCM) and Histogram of Oriented Gradients (HOG) features extraction is performed. Based on the features, LPDF-RVM is applied as a segmentation technique followed by GCNN. A detailed simulation analysis was carried out to highlight the better performance of the presented model.

## 2. RESEARCH ELABORATIONS

In the newly developed method, input image is pre-processed prior to perform image segmentation. Initially, normalization of input MR image is computed and proceed with further computation. The WF is employed for noise elimination and quantify the unclear images. Followed by, skull stripping is carried out for skull avoidance from MRI image and processed under the application of blob prediction and labeling models.

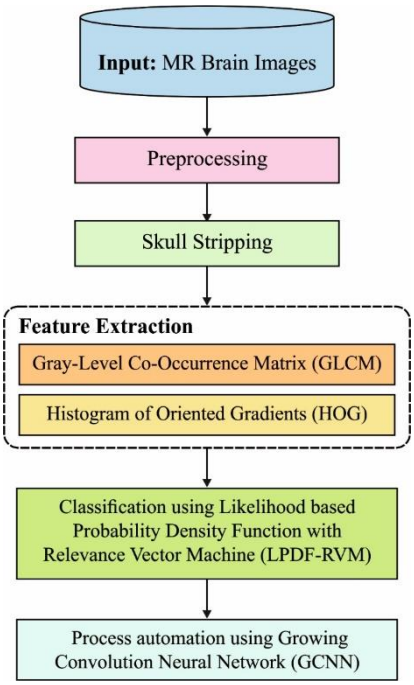


Fig. 1 Working process of proposed model

Once ROI has been identified, feature extraction is processed with the help of GLCM as well as HOG. According to the extracted features, LPDF-RVM has been employed for classification.

For making the feature classification and automation, GCNN is employed for automatic process. Fig. 1 depicts the flow diagram of newly deployed approach.

A. *Preprocessing*

Here, input image is preprocessed for eliminating the noise and uncertainties from image and proceed with further operations. In the preliminary phase, 3 steps have been followed: initially, Normalization is performed by using SEB approach. Followed by, WF is used for noise removal process. Then, skull stripping is one of the significant steps in BT segmentation.

B. *Feature Extraction*

In the newly developed approach, specific features are extracted from the preprocessed images namely,

- GLCM
- HOG

*1) Gray-Level Co-Occurrence Matrix (GLCM):* In this feature, texture is a major concern for developing significant representation of an image. GLCM feature extraction model is defined as a matrix form where the incidence of frequency of 2 pixels with specific intensities at distance d as well as angular orientation θ inside the image. Also, GLCM feature extraction is processed in 4 angular directions like 0°, 45°, 90°, 135°. Texture analysis is performed by considering grayscale features of an object for discriminating the objects. Thus, some of the extracted features are contrast, correlation, power, and homogeneity.

1. Contrast

It provides the value of intensity contrast among a pixel and neighbor of an image. Thus, contrast is described as:

$$Contrast = \sum_i \sum_j (i-j)^2 p(i,j) \quad (2)$$

Where p(i, j) implies the GLCM matrix.

2. Correlation

It is a value of measuring the pixel correlation to the neighbor of an image that is written as:

$$Correlation = \sum_i \sum_j \frac{ijp_d(i,j) - \mu_x \mu_y}{\sigma_x \sigma_y}) \quad (3)$$

Where$\mu_x, \mu_y$ and $\sigma_x, \sigma_y$ denotes the mean and Standard deviation (SD) of probability matrix GLCM with row-wise x as well as column-wise y.

3. Energy

The sum of squared units in GLCM is also named uniformity. Energy is illustrated as:

$$Energy = \sum_i \sum_j p^2(i,j) \quad (4)$$

4. Homogeneity

Homogeneity is the value of closeness of elements distribution in GLCM. Homogeneity value is maximum in images and similar to the grayness values that is explained as:

$$Homogeneity = \sum_i \sum_j \frac{p(i,j)}{1+|i-j|}) \quad (5)$$

*1) Histogram of Oriented Gradients (HOG):* The HOG is defined as a feature descriptor applied in computer vision as well as IP methodologies. Then, HOG is applied for extracting objects from applied images. It finds the shape and representation of an object by measuring the intensity gradients. The major principle behind HOG is local object form and shape of an image are illustrated by distribution of intensity gradients. Hence, image is classified as tiny connected regions named cells, and the pixels of a cell, HOG are induced. Followed by, descriptor is referred as combination of histograms. In case of enhanced accuracy, local histograms could be contrast-normalized by evaluating the intensity over huge scale image, named a block, and it is used for normalizing the cells.

a) Gradient Computation: HOG features are classifying the image window as tiny spatial regions named cells for a cell collecting local 1-D histogram of gradient directions across the pixels. Typically, the model applies 1-D centered, point discrete derivative mask of horizontal as well as vertical directions. Particularly, the model requires extraction of color information from an image from the filter kernels:

$$[-1, 0, 1\ ]\ and\ [-1, 0, 1]^T \tag{6}$$

Sampling the gradients are estimated under the application of Gaussian smoothing and various discrete derivative masks.

b) Orientation Binning: The HOG features, when a computation is completed, then the cell histograms are developed. A pixel estimates weighted vote to edge orientation histogram channel according to the orientation of gradient element and the votes are collected within the orientation bins across local spatial regions named as cells. Actually, the cells are rectangular or radial.

c) Descriptor Block: In gradient, efficiency has to be normalized locally, which needs accumulation of cells as huge scale and spatially connected blocks. Basically, HOG descriptor is the combination of vector and portion of normalized cell histograms from each block region. Thus, blocks which overlap refer to a cell contribution is excess and it is compared with final descriptor. There are 2 major blocks applied in Rectangular R-HOG blocks and circular C-HOG blocks. Here, R-HOG is applied to estimate the best parameters 2x2 cell blocks of 4x4 pixel cells along with histogram channels.

d) Block Normalization: In this module, there are 4 diverse models for block normalization. Consider V as non-normalized vector with histograms of provided block, $||^{v}||K$ is k-norm for k=1,2 and e is a tiny constant. Followed by, normalization factor is depicted as shown in the following:

$$L2-norm\ :\ f\frac{v}{\sqrt{||v||_2^2+e^2}} \tag{7}$$

L2-norm and clipping (reducing the high values of v to 0.2) and renormalizing is illustrated by,

$$L1-norm\ :\ f=\frac{v}{||v||_{1+e}} \tag{8}$$

$$L1-sqrt:\ f=\sqrt{\frac{v}{||v||_{1+e}}} \tag{9}$$

C. *Segmentation*

*1) Likelihood based Probability Density Function with Relevance Vector Machine (LPDF-RVM):* Once the feature extraction is completed, image segmentation is carried out and divided

into infected and non-infected portion. Under the application of LPDF-RVM, classification is performed. The working function of original RVM by means of sparsity is computed by image smoothness [14]. Therefore, inexistence of explicit prior structure across the weight variance refers that sparsity is based on the choice of kernel functions and parameters. As a result, overfitting and under fitting issues have emerged. In order to overcome the problem, LPDF-RVM method has been applied. Moreover, maximum likelihood function is applied for gaining optimal hyper parameters and allocates 0 to the weights based on the hyper parameters to make sure the sparsity of model. For example, a sample set $(x_1, x_2.,..,x_n$ , ), where $y_i \in \{+1, -1\}$ implies the class label of a sample, the scheme of RVM is illustrated as shown below:

$$y(x) = \sum_{n1}^{N} w_n K(x, x_n) + w_0 \quad (10)$$

Where K(,) defines the kernel function and $w_n$ implies the weight of samples. In addition, RVM applies a Bernoulli distribution for developing PDF as:

$$p(t_i|x) = N(t_i|y(x_i; w), \sigma^2) \quad (11)$$

Where the desired value is p($t_i|x$) as well as the variance is $\sigma^2$.

To eliminate over-fitting, the newly developed model is applied and illustrated as:

$$p(x_i|\mu) = \prod_{i=1}^{N} p(x_i|\mu) = (2\pi\sigma^2)^{-\frac{n}{2}} exp\,(-\frac{1}{2\sigma^2}\sum_{i=1}^{n}(x_i - \mu)^2) \quad (12)$$

Where, the function $p(x_i|\mu)$ is applied to mark the fact where the density is based on the unknown parameter $\mu$ denotes the normal distribution.

When classification process is implemented, the posterior probability of weights cannot be estimated. Therefore, Laplacian theory is applied to approximate the estimation: for recently developed $\alpha$, identify the possible weight $w_{MP}$ . Apply the 2nd order Newton model in (13) to accomplish $w_{MP}$

$$log\{p(t|w)\ P(x_i|\mu)\} = \sum_{n=1}^{N}[t_n log y_n + (1 - t_n) log(1 - y_n)] - \frac{1}{2}w^T \mu w \quad (13)$$

Where,

$$y_n = \sigma\{y(x_n; w)\}$$

Under the Laplacian model, log posterior probability is normalized. Followed by, considering the derivatives on (13) intends to derive the given expression:

$$\nabla_w \nabla_w log p(w|t, \mu)|_{w_{MP}} = -(\varphi^T|B\varphi + \mu) \quad (14)$$

Where, $\varphi = [\varphi(x_1), \varphi(x_2), .., \varphi(x_N)]^T$ and B=diag ($\beta_1, \beta_2, .. \beta_n$).

Apply (5) for accomplishing the covariance matrix $\sum$ . Then, upgrade the hyper parameter. The model performance described by relevance vector is defined as high-dimensional hyperplane, which approximates the test samples of the plane.

*2) Growing Convolution Neural Network (GCNN):* When the features are divided for making automation, apply DL model GCNN. It enables the encoding features from inputs, enhances the upcoming function, and limit the count of parameters for the system with complicated applications. With no change in organization of input GCNN trained to diverse process with the application of generic characteristics. On the other hand, the difference between NN and GCNN is the capability of dynamically extension of network has relied on the rules. Firstly, the number of layers such as CONV, RELU, &amp, POOL required to be described [15]. Afterward, the system expanded independently in interactive fashion, with Backpropagation (BP) accessible on fixed edges as well as nodes of diverse layers. The

network will be trained and the feedback processed from BP for collective filters till reaching the already existing threshold value for accuracy. When the complete error of a system, network concentrates on minimal value of edges. Therefore, training process is extended for growing algorithm in error confluence speed is changed to minimum threshold value. Finally, the GCNN system is overworked prior to initializing segmentation and makes the network topology in dynamic fashion.

## 3. RESULTS OR FINDING

The experimental analysis is performed using MATLAB tool. The database is used for BRAINIX medical images. The performance of the presented LPDF-RVM approach is related to Random Forest (RF) with GCNN with respect to accuracy, precision, recall, and Peak Signal-to-Noise Ratio (PSNR).

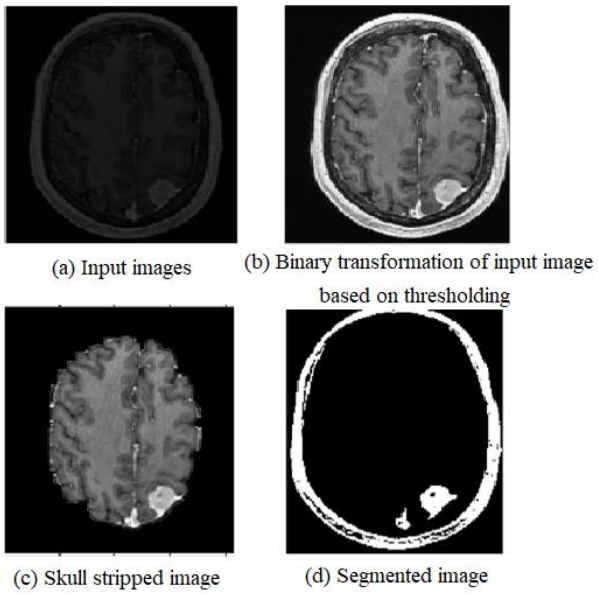


Fig. 2 Segmentation results

Fig. 2 illustrates the outcome of the presented technique. Initially, the Brain MR images are taken as input. Fig. 2(b) shows the Binary transformation of input image based on thresholding. Fig. 2(c) represents the Skull stripping image. Finally, the segmented images are obtained using LPDF-RVM which is shown in Fig. 2(d).

Table 2 examines the result analysis of proposed LPDFRVM-GCNN model with different measures interms of precision, recall, accuracy, and PSNR.

Table 1: Result analysis of Existing with Proposed LPDFRVM-GCNN Method

| **Measures** | **RF-GCNN** | **LPDFRVM-GCNN** |
|---|---|---|
| Precision | 98.00 | 98.50 |
| Recall | 98.23 | 98.65 |
| Accuracy | 98.00 | 98.50 |

| | | |
|---|---|---|
| PSNR | 96.64 | 97.00 |

A. Accuracy

Accuracy is an important measure that defines the overall efficiency of the model and is defined by

$$Accuracy = \frac{T_p + T_n}{(T_p + T_n + F_p + F_n)} \quad (15)$$

The performance of the proposed LPDF-RVM and GCNN scheme is compared with RF with GCNN in terms of accuracy as depicted in Fig. 3. These approaches are plotted along the x-axis and accuracy is plotted along the y-axis. As observed from the results, it can be finally reported that the novel LPDF-RVM attains better accuracy performance in comparison with the available system.

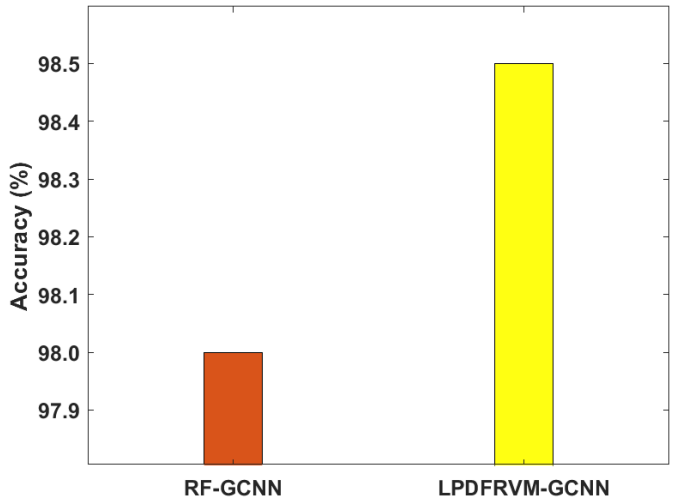


Fig. 3 Accuracy comparison

B. Precision

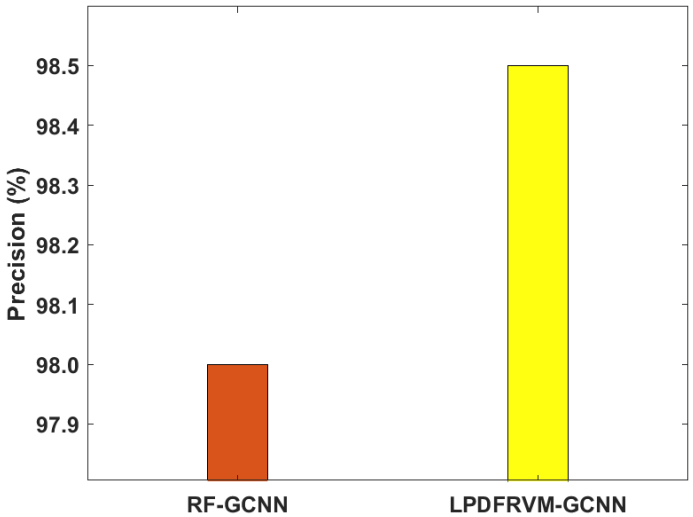


Fig. 4 Precision comparison

Precision is determined by

$$Precison(P) = \frac{T_p}{T_p + F_p} \tag{16}$$

The precision of the proposed LPDF-RVM and GCNN scheme is compared with RF with GCNN. The models are plotted along the x-axis and precision is plotted along the y-axis. Fig. 4 illustrates the precision taken by several techniques. Since the data, it has been cleared that the presented model carried out better and further effectual to the other mentioned technique.

C. Recall

The recall is ratio of correctly forecasted positive observations to every observation in actual class - yes. It can be calculated as:

$$Recall\ (R) = \frac{T_p}{T_p + F_n} \tag{17}$$

Fig. 5 shows the comparative analysis of recall performance of the proposed LPDF-RVM and GCNN scheme is compared with RF with GCNN method. The existing and projected techniques are plotted along the x-axis and recall is plotted along the y-axis. The results obtained from the experiments reveal that the newly established scheme attains much better recall in comparison with the earlier techniques.

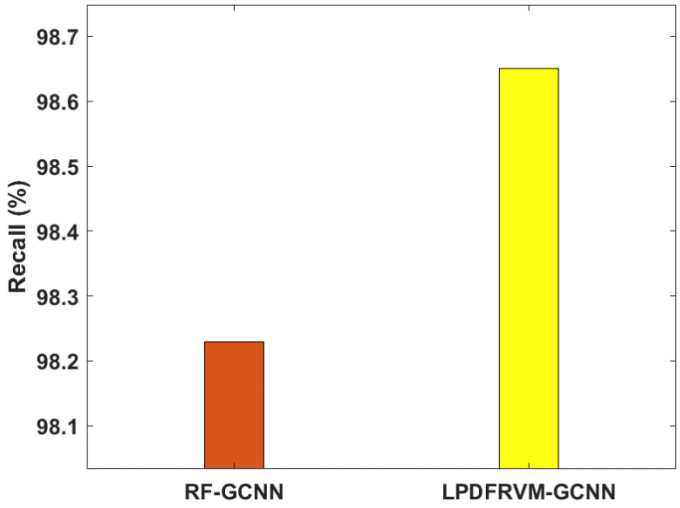


Fig. 5 Recall comparison

D. PSNR comparison

The PSNR is used to measure the quality of the images. It is represented as:

$$PSNR = 10 \cdot \log_{10}\left(\frac{255^2}{MSE}\right)[dB] \tag{18}$$

The PSNR of the proposed and existing methods are compared with are shown in Fig. 6. The existing and presented techniques are plotted along the x-axis and PSNR is plotted along the y-axis. From the experimental outcomes, it is concluded that the presented system achieves higher PSNR value related to the previous technique.

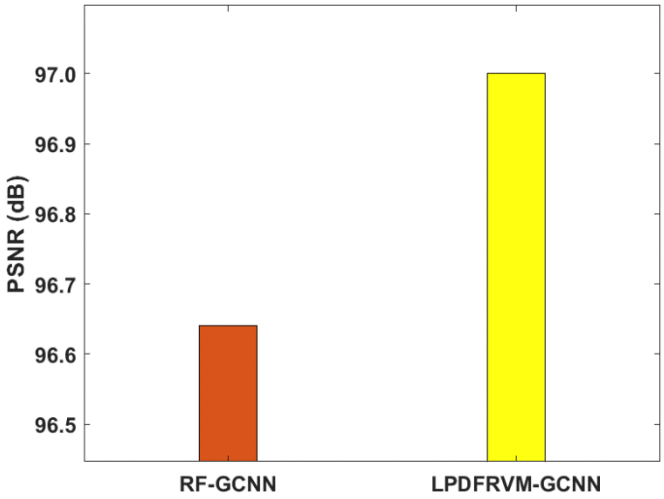


Fig. 6 PSNR comparison

## 4. CONCLUSIONS

The presented system designed LPDF-RVM and GCNN for automatic BT segmentation. To eliminate the noise and improve the performance, WF is applied. After the completion of skull stripping, GLCM and HOG features extracted to improve the classification accuracy. Then LPDF-RVM is utilized to classified the feature to their respective classes. When the features are classified to automate the procedure, utilize DL model GCNN. The experimental outcomes illustrate the presented method achieves optimal performance relates to the previous methods with respect to accuracy, precision, recall, and PSNR.

## 5. REFERENCES

[1] Pereira, S., Pinto, A., Alves, V., & Silva, C. A. (2016). BT segmentation using convolutional neural networks in MRI images. IEEE transactions on medical imaging, 35(5), 1240-1251.
[2] Zhuge, Y., Krauze, A. V., Ning, H., Cheng, J. Y., Arora, B. C., Camphausen, K., & Miller, R. W. (2017). BT segmentation using holistically nested neural networks in MRI images. Medical physics, 44(10), 5234-5243.
[3] Bauer, S.; Wiest, R.; Nolte, L.-P.; Reyes, M. A survey of MRI-based medical image analysis for BT studies. Phys. Med. Biol. 2013.
[4] Zhao, X.; Wu, Y.; Song, G.; Li, Z.; Zhang, Y.; Fan, Y. A deep learning model integrating FCNNs and CRFs for BT segmentation. Med. Image Anal. 2018, 43, 98–111.
[5] Logeswari, T.; Karnan, M. An improved implementation of BT detection using segmentation based on hierarchical self organizing map. Int. J. Comput. Theory Eng. 2010, 2, 591.
[6] Dong, H., Yang, G., Liu, F., Mo, Y., & Guo, Y. (2017, July). Automatic BT detection and segmentation using U-Net based fully convolutional networks. In annual conference on medical image understanding and analysis (pp. 506-517). Springer, Cham.
[7] Zhang, N., Ruan, S., Lebonvallet, S., Liao, Q., & Zhu, Y. (2011). Kernel feature selection to fuse multi-spectral MRI images for BT segmentation. Computer Vision and Image Understanding, 115(2), 256-269.

[8] Rajendran, A., & Dhanasekaran, R. (2012). Fuzzy clustering and deformable model for tumor segmentation on MRI brain image: a combined approach. Procedia Engineering, 30, 327-333.
[9] Aslam, E. Khan, and M.M.S. Beg, Improved edge detection algorithm for BT segmentation, Elsevier, 58 (2015), pp. 430–437.
[10] Aina, A. Jaffar, and T. SunChoic. Fuzzy anisotropic diffusion based segmentation and Texture based ensemble classification of BT, Appl Soft Comput 21, (2014), 330–340.
[11] Diaz and P. Boulanger, "Atlas to patient registration with BT based on a mesh-free method," In 37th annual international conference of the IEEE engineering in medicine and biological society, 2015.
[12] Dou, W, Ruan, S, Chen, Y, Bloyet, D & Constans, J. M. 2007, 'A framework of fuzzy information fusion for the segmentation of BT tissues on MR images'. Image and vision Computing, vol.25, no. 2, pp. 164-171.
[13] Mittal, M., Goyal, L. M., Kaur, S., Kaur, I., Verma, A., & Hemanth, D. J. (2019). Deep learning based enhanced tumor segmentation approach for MR brain images. Applied Soft Computing, 78, 346-354.
[14] Liu, X., Chen, X., Li, J., Zhou, X., & Chen, Y. (2020). Facies identification based on multikernel relevance vector machine. IEEE Transactions on Geoscience and Remote Sensing.
[15] Brinker, T. J., Hekler, A., Utikal, J. S., Grabe, N., Schadendorf, D., Klode, J., ... & von Kalle, C. (2018). Skin cancer classification using convolutional neural networks: systematic review. Journal of medical Internet research, 20(10), e11936.
[16] K. Shankar, Lakshmanaprabu S. K, Ashish Khanna, Sudeep Tanwar, Joel J.P.C.Rodrigues, Nihar Ranjan Roy, "Alzheimer detection using Group Grey Wolf Optimization based features with convolutional classifier", Computers & Electrical Engineering, Volume 77, Pages 230-243, July 2019.
[17] Lakshmanaprabu S.K, Sachi Nandan Mohanty, Sheeba Rani S, Sujatha Krishnamoorthy, Uthayakumar J, K. Shankar, "Online clinical decision support system using optimal deep neural networks", Applied Soft Computing, Volume 81, Page(s): 1-10, August 2019.
[18] Lakshmanaprabu S.K, Sachi Nandan Mohanty, K. Shankar, Arunkumar N, Gustavo Ramireze, "Optimal deep learning model for classification of lung cancer on CT images", Future Generation Computer Systems, Volume 92, Pages 374-382, March 2019.
[19] Joshua Samuel Raj, S. Jeya Shobana, Irina Valeryevna Pustokhina, Denis Alexandrovich Pustokhin, Deepak Gupta, K. Shankar, "Optimal Feature Selection based Medical Image Classification using Deep Learning Model in Internet of Medical Things", IEEE Access, Volume: 8, Issue:1, Page(s): 58006-58017, December 2020.
[20] Mohamed Elhoseny, Gui-Bin Bian, SK. Lakshmanaprabu, K. Shankar, Amit Kumar Singh, Wanqing Wu, "Effective Features to Classify Ovarian Cancer Data in Internet of Medical Things", Computer Networks, Volume 159, Pages 147-156, August 2019.
[21] K. Shankar, Abdul Rahaman WahabSait, DeepakGupta, S.K.Lakshmanaprabu, Ashish Khanna, Hari Mohan Pandey, "Automated Detection and Classification of Fundus Diabetic Retinopathy Images using Synergic Deep Learning Model", Pattern Recognition Letters, Volume 133, Pages 210-216, May 2020.